Nuclear Quadrupole Coupling Tensors of ^2H in the α-Alum $RbAl(SO_4)_2 \cdot 12D_2O$ and the Dynamical Behaviour of the D_2O Molecules. An Investigation by NMR and IR *

J. Ramakrishna [a], Norbert Weiden [b], and Alarich Weiss [b]

[a] Department of Physics, Indian Institute of Science, Bangalore-560 012, India
[b] Institut für Physikalische Chemie, Technische Hochschule Darmstadt, D-6100 Darmstadt

Z. Naturforsch. **45a**, 511–518 (1990); received August 21, 1989

By single crystal NMR the nuclear quadrupole coupling constants $eQ\Phi_{zz}h^{-1}(^2H)$, the asymmetry parameters $\eta(^2H)$ and the dircetion cosines of the principal axes of the electric field gradient tensors of the ^2H atoms of the two kinds of D_2O molecules have been determined at 295 K in $RbAl(SO_4)_2 \cdot 12D_2O$. The results show that the D_2O molecules surrounding the ion Al^{3+} are "static" within the time scale of the ^2H nuclear quadrupole interaction while the D_2O belonging to the octahedron around the Rb^+ undergoes fast reorientations around the twofold molecular axis. For the two kinds of D_2O in the alum we found: $eQ\Phi_{zz}^{(1)}h^{-1}(^2H)=186.5$ kHz, $\eta^{(1)}(^2H)=0.1234$; $eQ\Phi_{zz}^{(2)}h^{-1}(^2H)=169.7$ kHz, $\eta^{(2)}(^2H)=0.1297$; $eQ\Phi_{zz}^{(3)}h^{-1}(^2H)=122.1$ kHz, $\eta^{(3)}(^2H)=0.8087$. $eQ\Phi_{zz}^{(1)}$ and $eQ\Phi_{zz}^{(2)}$ belong to the "static" D_2O molecules and an assignment to the two different ^2H atoms has been performed. The IR spectra of $RbAl(SO_4)_2 \cdot 12(H_{1-x}D_x)_2O$ have been investigated, and for the O–D stretching frequencies values of 2145 cm^{-1}, 2235 cm^{-1}, 2470 cm^{-1} and 2525 cm^{-1} have been obtained. They agree well with the relations between $\tilde{\nu}_{OD}$ and $eQ\Phi_{zz}h^{-1}(^2H)$ given in the literature.

Introduction

Alums have the chemical composition $Me^+Me^{3+}(RX_4)_2^{2-} \cdot 12H_2O$ where $Me^+ = Na^+$, K^+, NH_4^+, Rb^+, Cs^+, Tl^+, $H_2NNH_3^+$, $CH_3NH_3^+$ ... and $Me^{3+} = Al^{3+}$, Ga^{3+}, In^{3+}, Fe^{3+}, Cr^{3+} .... The anion RX_4^{2-} may be SO_4^{2-}, SeO_4^{2-} or BeF_4^{2-}. Though all the alums crystallize in the cubic space group T_h^6-Pa 3 with $Z=4$, α-, β-, and γ-alums are distinguished, based on differences in the arrangement of the RX_4^{2-} ions. A series of alums has been investigated, using NMR and NQR, to obtain information on the electric field gradient (EFG) at the sites of Me^+ and Me^{3+}, on internal motions and on the temperature dependence of the EFG (see e.g. [1]–[9]). The ions Me^+ and Me^{3+} are surrounded by an octahedron of six water molecules, and a complex network of H-bonds is one of the main features of the structure of the alums.

H-bonds have been object of investigation for many years, using a variety of spectroscopic and diffraction techniques. The first study using NMR in this direction was by Pake [10] on $CaSO_4 \cdot 2H_2O$. Ketudat and Pound [11] from their experiments on ^2H NMR in three crystal hydrates demonstrated the main features that can be learnt from ^2H NMR in single crystals of hydrates, and since that time a large number of crystal hydrates has been investigated (for a survey see [12]). The full power of ^2H and ^1H NMR in solid state research is however achievewd only in combination with results from other methods, particularly X-ray and neutron diffraction and infrared spectroscopy.

The first attempt to record an ^2H NMR spectrum in alums was made by Ketudat [13] in $KAl(SO_4)_2 \cdot 12D_2O$ at 108 K. He states that at least some of the water molecules are "static" at that temperature. However it was not possible for him to assign the lines of the spectrum and to calculate the nuclear quadrupole coupling constant (NQCC) $e^2qQ\Phi_{zz}h^{-1}(^2H)$, the asymmetry parameter $\eta(^2H)$ and the direction cosines of the principal axes of the EFG tensor at the ^2H site. In this paper we report a study of ^2H NMR in $RbAl(SO_4)_2 \cdot 12D_2O$ (α-type alum) at room temperature.

* Presented at the Xth International Symposium on Nuclear Quadrupole Resonance Spectroscopy, Takayama, Japan, August 22–26, 1989.

Reprint requests to Prof. Dr. Al. Weiss, Institut für Physikalische Chemie, Technische Hochschule Darmstadt, Petersenstraße 20, D-6100 Darmstadt.

0932-0784 / 90 / 0300-0511 $ 01.30/0. – Please order a reprint rather than making your own copy.

Experimental

Large single crystals of about 1.5 cm^3 volume have been grown by slow cooling (cooling rate 0.05 K/h) of a saturated solution of $RbAl(SO_4)_2$ in D_2O. The crystals were optically transparent and developed mainly the faces {111} and – much smaller – faces {110} and {100}.

To obtain the angular dependence of the satellite splitting of the ^2H NMR spectra a single crystal of $RbAl(SO_4)_2 \cdot 12\,D_2O$ has been alinged optically on a one circle goniometer in such a way that it could be rotated in the magnetic field $\boldsymbol{B}_0$ around the axis [100] $\perp \boldsymbol{B}_0$. A second crystal has been oriented for the rotation around the axis [110] $\perp \boldsymbol{B}_0$ and a third for [111] $\perp \boldsymbol{B}_0$.

The spectra have been recorded using a Varian WL 200 wideline spectrometer by slowly varying the magnetic field over a range of 0.04 T in 16 min. The oscillator frequency has been stabilized to 8.5000 MHz $\pm$ 0.000001 MHz using an external frequency synthesizer. Lock-in technique with a time constant of 3 s has been applied together with signal averaging in order to obtain a signal to noise ratio of at least 5 even for the weakest signals. During the measurements the room temperature has been kept constant at (295 $\pm$ 0.5) K.

Results

$RbAl(SO_4)_2 \cdot 12\,D_2O$ belongs to the alums of α-type. In Fig. 1 a sketch of the unit cell, which contains 48 water molecules, is shown. The aluminum ion is surrounded by an almost regular octahedron of six crystallographically equivalent water molecules which occupy position 24 d with point symmetry 1. The rather distorted water octahedron around the rubidium ion is also built up from crystallographically equivalent water molecules. Even though there are only two crystallographically inequivalent kinds of D_2O molecules in the unit cell (2 times in 24 d), for a general orientation of the crystal with respect to $\boldsymbol{B}_0$ the existence of 96 deuterons in the unit cell may lead to the appearance of 96 satellite lines in the NMR spectrum. For special orientations this number can be reduced due to the symmetry of the lattice but nevertheless the spectra are rather complex, as shown in Fig. 2 for a few examples. These spectra also illustrate the common features of all ^2H NMR spectra obtained

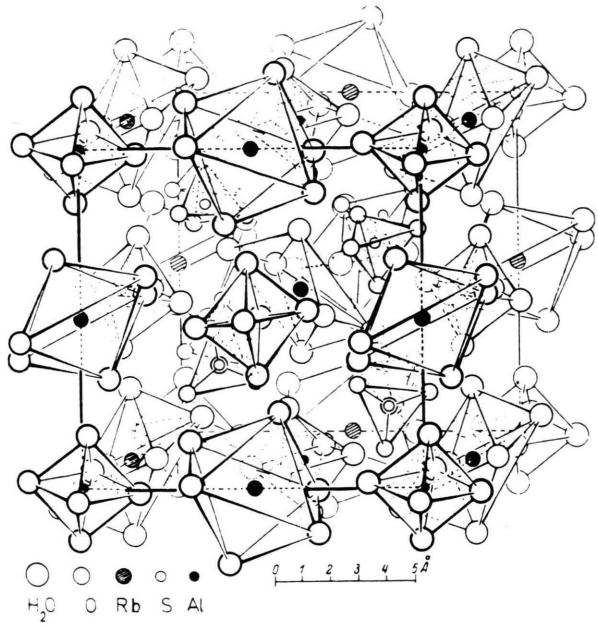

Fig. 1. Sketch of the unit cell of the α-alums.

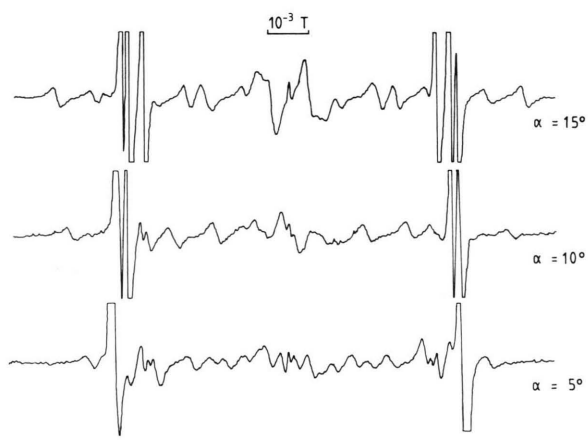

Fig. 2. Three representative NMR spectra of $RbAl(SO_4)_2 \cdot 12\,D_2O$ for rotation around the axis [100]. α is the angle between the crystal axis $\boldsymbol{a}$ and the magnetic field $\boldsymbol{B}_0$. $T = 295$ K.

at room temperature. First, there is a severe overlapping of lines and, secondly, there are two kinds of signals – one set of weak signals and another one of rather strong signals.

To obtain $eQ\Phi_{zz}h^{-1}(^2H)$, $\eta(^2H)$, and the direction cosines of the principal axes of the EFG tensor Φ_{xx}, Φ_{yy}, Φ_{zz} the crystal has been rotated in a first run around the axis [100]. The data have been analysed

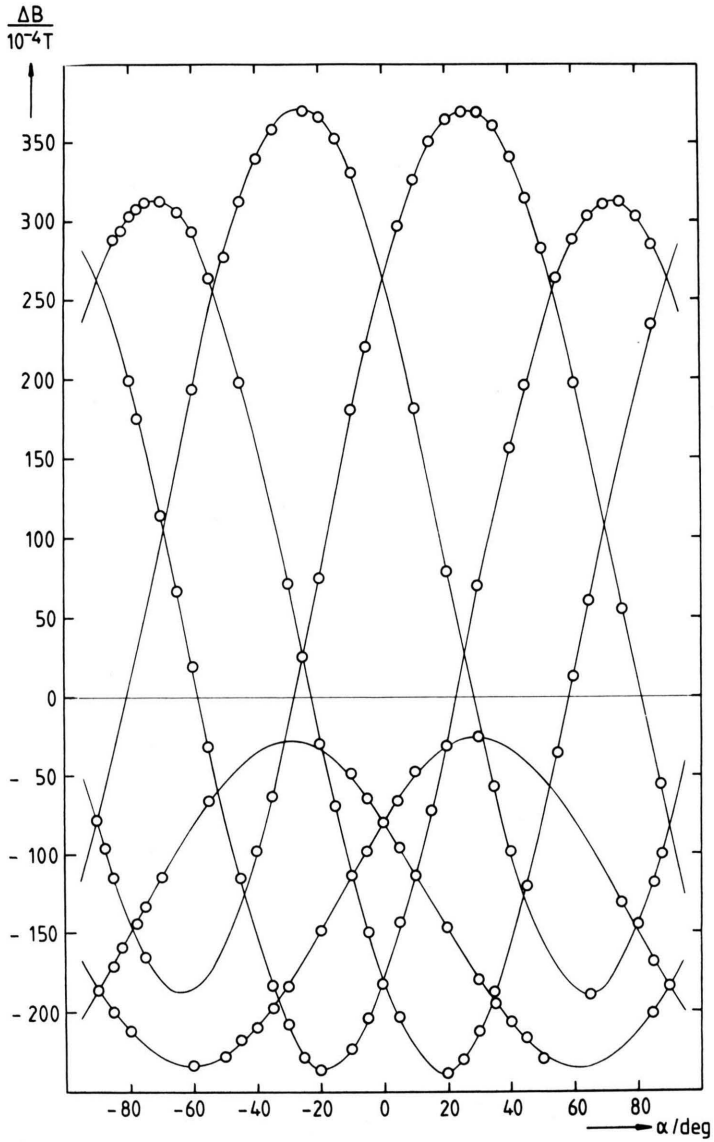

Fig. 3. Set 1 of six curves fitting part of the experimental values for the satellite splitting of the weak signals. Rotation axis is [100]. α is the angle between the crystal axis $\boldsymbol{a}$ and the magnetic field $\boldsymbol{B}_0$. ΔB is the satellite splitting. $T = 295$ K.

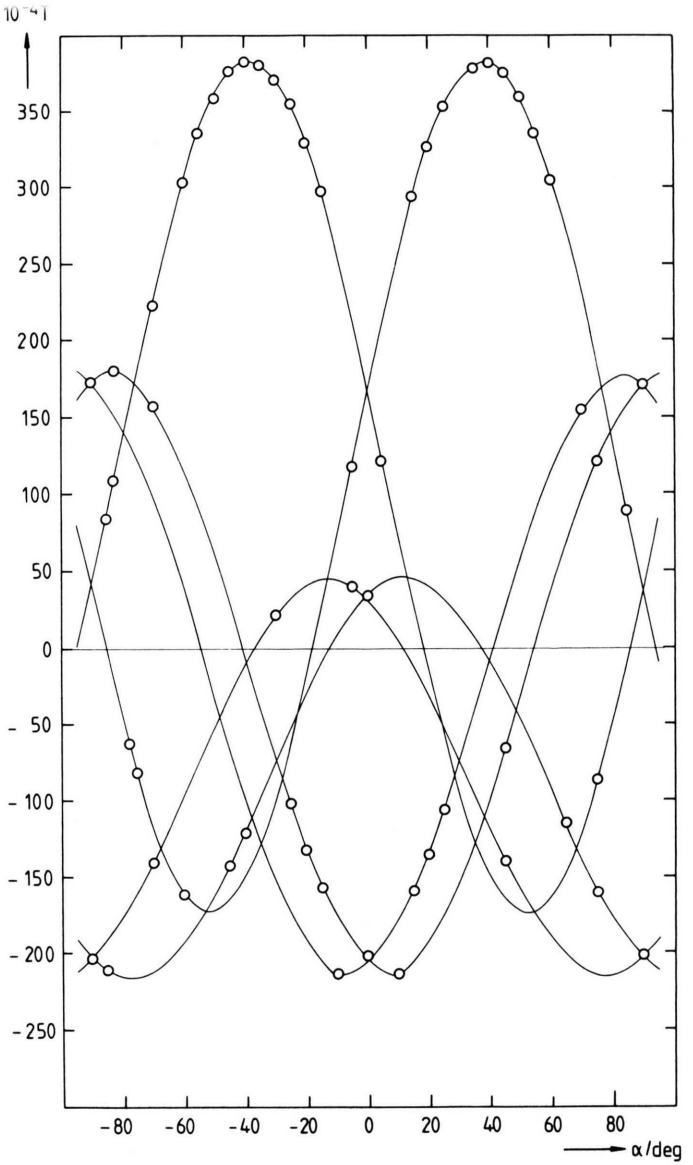

Fig. 4. Set 2 of six curves fitting part of the experimental values for the satellite splitting of the weak signals. Rotation axis is [100]. α is the angle between the crystal axis $\boldsymbol{a}$ and the magnetic field $\boldsymbol{B}_0$. ΔB is the satellite splitting. $T = 295$ K.

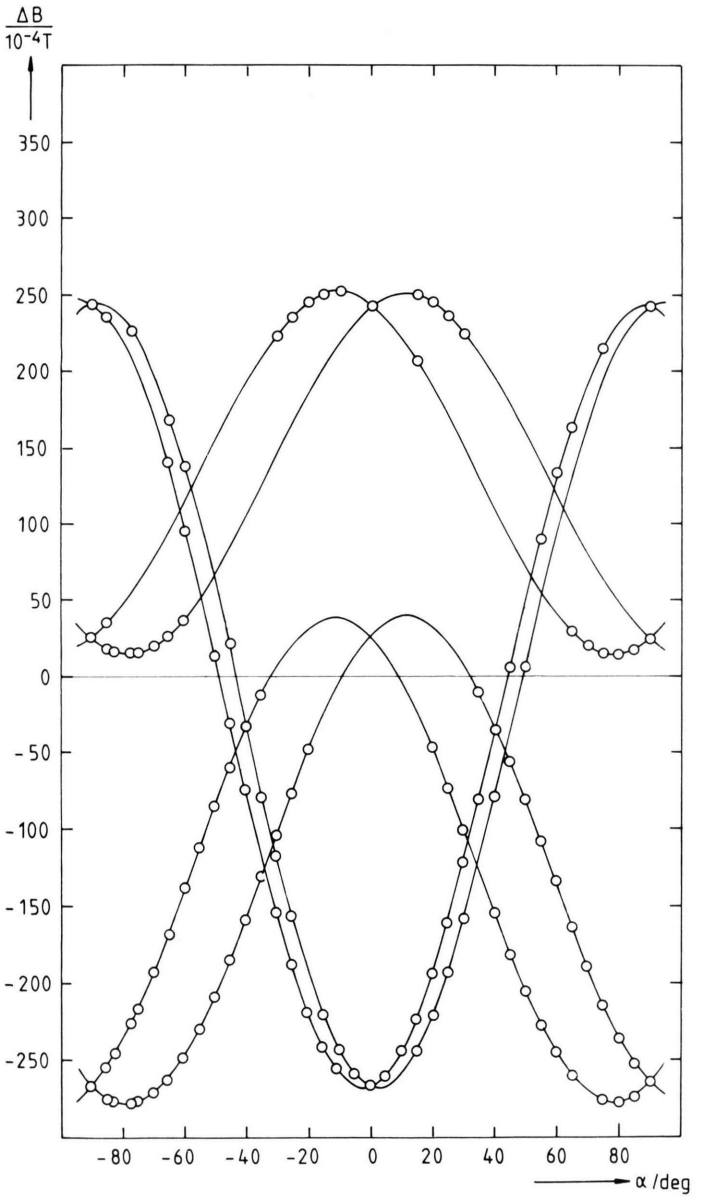

Fig. 5. Set 3 of six curves fitting the experimental values for the satellite splitting of the strong signals. Rotation axis is [100]. α is the angle between the crystal axis $\boldsymbol{a}$ and the magnetic field $\boldsymbol{B}_0$. ΔB is the satellite splitting. $T = 295$ K.

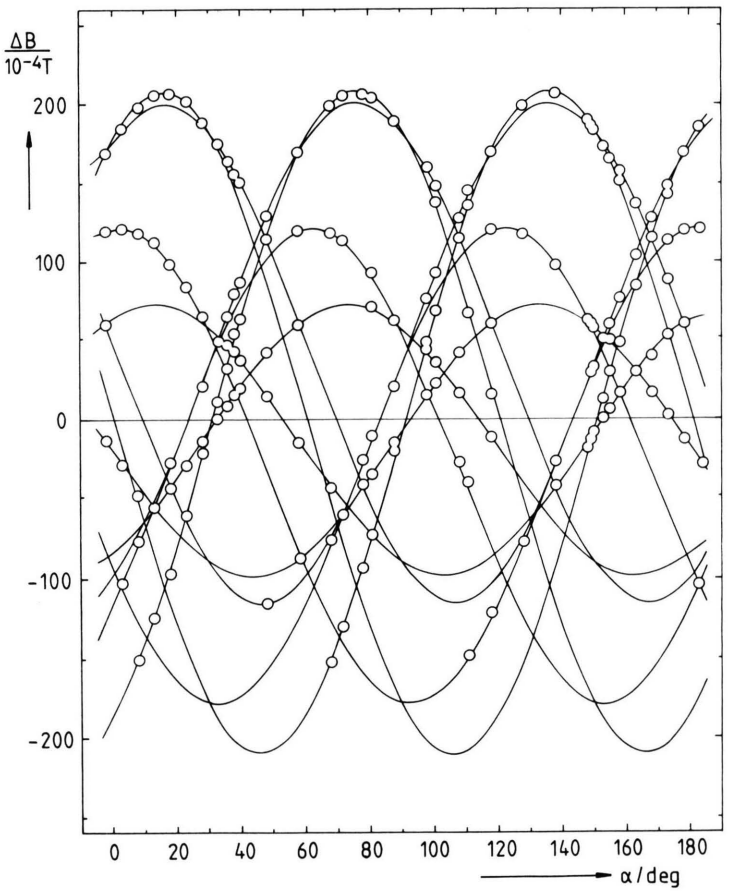

Fig. 6. Fit of the experimental points for rotation around the axis [111] with the results of solution (a) for set 3 of Tables 1 and 2. Only the data for the splittings of the strong signals are shown. $T = 295$ K.

Table 1. The two solutions (a) and (b) obtained due to the uncertainty in Volkoff's method for the asymmetry parameter $\eta(^2H)$ and the nuclear quadrupole coupling constant $eQ\Phi_{zz}h^{-1}(^2H)$ for each of the three sets of six curves shown in Figs. 3, 4, 5. The solutions (a) turned out to be the correct ones. $T = 295$ K.

Solution		(a)	(b)
Set 1	$eQ\Phi_{zz}h^{-1}(^2H)$/kHz	186.5	170.6
	$\eta(^2H)$	0.1234	0.7549
Set 2	$eQ\Phi_{zz}h^{-1}(^2H)$/kHz	169.7	166.0
	$\eta(^2H)$	0.1297	0.3921
Set 3	$eQ\Phi_{zz}h^{-1}(^2H)$/kHz	122.1	122.7
	$\eta(^2H)$	0.8087	0.7858

Table 2. Direction cosines λ, μ, ν of the principal axes $\Phi_{xx}^{(j)}$, $\Phi_{yy}^{(j)}$, and $\Phi_{zz}^{(j)}$, $j = 1, 2, 3$ of the EFG tensors with respect to the crystal axes for solutions (a) of Table 1. $T = 295$ K.

		λ	μ	ν
Set 1	$\Phi_{xx}^{(1)}$	.16910	.48484	.85809
	$\Phi_{yy}^{(1)}$	−.94260	−.17482	.28452
	$\Phi_{zz}^{(1)}$	.28795	−.85696	.42745
Set 2	$\Phi_{xx}^{(2)}$	−.31990	.61580	−.72004
	$\Phi_{yy}^{(2)}$	−.93995	−.11077	.32285
	$\Phi_{zz}^{(2)}$	.11905	.78007	.61425
Set 3	$\Phi_{xx}^{(3)}$	.21496	.95800	−.18977
	$\Phi_{yy}^{(3)}$	−.97638	.20640	−.06401
	$\Phi_{zz}^{(3)}$	−.02215	.19904	.97974

following the method of Volkoff and coworkers [14]. Due to the large number of lines and their overlapping, this turned out to be a very complex and puzzling job, leading to 18 curves of the form $\Delta B = A + B\cos(2\alpha) + C\sin(2\alpha)$. With the aid of Volkoff's relations for the coefficients A and B and the different intensities, the 18 curves could be split up into 3 sets, each of 6 curves. The three sets of curves are shown in Figs. 3, 4 and 5. The first set of 6 curves (Fig. 3) fits part of the weak signals and belongs, as can be seen, to two groups of symmetry related deuterons. The second set fits the remaining part of the weak signals of another two groups of symmetry related deuterons. The third set fits the strong signals, again consisting of two groups of symmetry related curves.

Using as example $CaSO_4 \cdot 2D_2O$, Hutton and Peterson [15] have shown that the Volkoff method does not lead to a unique solution for the EFG tensor if the nuclei under consideration are located at symmetry related but magnetically inequivalent sites. We have also obtained two solutions for each set, for which $\eta(^2H)$ and $eQ\Phi_{zz}h^{-1}(^2H)$ are given in Table 1. Comparison of the results with data for other crystal hydrates in [12] leads to the conclusion that sets 1 and 2 belong to "static" D_2O molecules and set 3 to flipping ones. In addition, the η values show that for sets 1 and 2 the solution (a) are the correct ones. The direction cosines of $\Phi_{xx}^{(j)}$, $\Phi_{yy}^{(j)}$, and $\Phi_{zz}^{(j)}$, $j = 1, 2$, with respect to the crystal axes for the solutions (a) of sets 1 and 2 are given in Table 2. The angle between the principal axes Φ_{zz} turned out to be 111.8°, indicating that they belong to the same water molecule.

The situation for set 3 is more complicated, and more experimental data had to be obtained before deciding which of the very similar solutions is the correct one. We have collected data for the rotation of the crystal around the axis [110]. Unfortunately this did not help, due to severe overlapping of the resonance lines. As a next step, the crystal has been rotated around [111] and Fig. 6 shows the result of fitting the experimental data taking solution (a) of set 3, which turns out to be the correct one. The mismatch for solution (b) is about 5 kHz at the top of the curves. The direction cosines of $\Phi_{xx}^{(3)}$, $\Phi_{yy}^{(3)}$, and $\Phi_{zz}^{(3)}$ are given in Table 3, too.

Discussion

Larson and Cromer [16] have refined the crystal structure of the α-alums $Me^{1+}Al(SO_4) \cdot 12H_2O$, $Me^{+1} = K$, NH_4 and Rb using single crystal X-ray diffraction data, while the structure of $ND_4Al(SO_4)_2 \cdot 12D_2O$ has been determined by Cromer and Kay [17] using three dimensional neutron diffraction data leading to the determination of the deuteron positions. The lattice constants of the protonated Rb- and NH_4-alum are 1224.3 ± 0.3 pm and 1224.0 ± 0.3 pm, respectively, while that of ND_4-alum is 1224.3 ± 0.1 pm, showing on the one hand that there is little isotope effect and on the other hand that the lattice constants of Rb- and NH_4-alum are the same within the limits of experimental error. This holds also for the position of the atoms in the whole unit cell of the two alums, as can be seen from the atomic positions, interatomic distances and bond angles. Also the H-bonds are almost the same length in the two cases. In Fig. 7a projection of a part of the structure onto the plane of

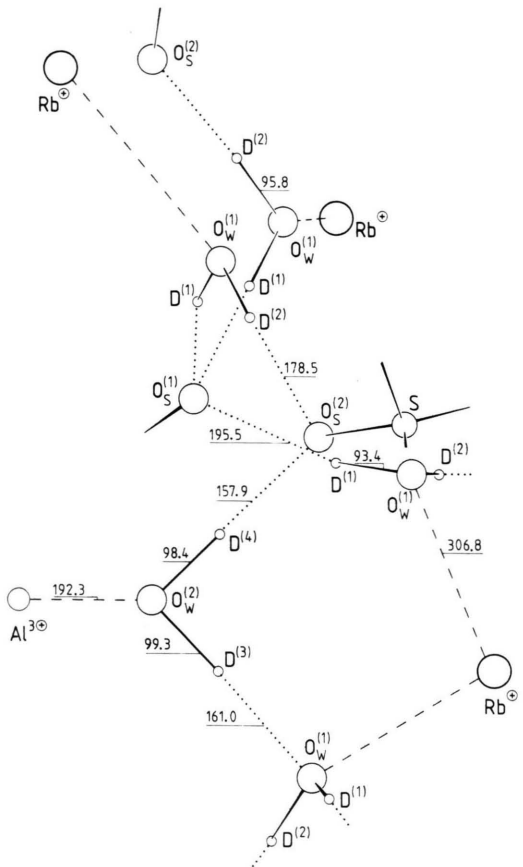

Fig. 7. Projection of a part of the unit cell of $RbAl(SO_4)_2 \cdot 12\,D_2O$ onto the plane of a water molecule $D^{(3)}-O_w^{(2)}-D^{(4)}$ belonging to the water octahedron around the ion Al^{3+}. All distances are given in pm. The numbering of the atoms corresponds to that of the crystal structure determination [17].

$\sphericalangle(\Phi_{zz}^{(1)}, \Phi_{zz}^{(2)})$	$= 111.8°$
$\sphericalangle(D^{(3)}-O_w^{(2)}-D^{(4)})$	$= 108.2°$
$\sphericalangle(\Phi_{zz}^{(1)}, O_w^{(2)}-D^{(4)})$	$= 2.2°$
$\sphericalangle(\Phi_{zz}^{(2)}, O_w^{(2)}-D^{(3)})$	$= 2.3°$
$\sphericalangle(\Phi_{yy}^{(1)}, \Phi_{yy}^{(2)})$	$= 4.3°$
$\sphericalangle(\Phi_{yy}^{(1)}, \boldsymbol{n}^{(2)})$	$= 5.1°$
$\sphericalangle(\Phi_{yy}^{(2)}, \boldsymbol{n}^{(2)})$	$= 4.0°$

Table 3. Angles between the principal axes $\Phi_{jj}^{(1)}$ and $\Phi_{jj}^{(2)}$, $j=x, y, z$, and angles they form with structure elements of the molecule $D^{(3)}-O_w^{(2)}-D^{(4)}$. $\boldsymbol{n}^{(2)}$ = normal of the molecular plane. $T=295$ K.

Table 4. Orientation of the principal axes of $\Phi_{jj}^{(3)}$, $j=x, y, z$, with respect to the water molecule $D^{(1)}-O_w^{(1)}-D^{(2)}$, which belongs to the octahedron around Rb^+. $\boldsymbol{n}^{(1)}$ is the normal of the plane of the molecule. $T=295$ K.

$\sphericalangle(\Phi_{zz}^{(3)}, \boldsymbol{n}^{(1)})$	$= 2.2°$
$\sphericalangle(\Phi_{yy}^{(3)}, D^{(1)}-D^{(2)})$	$= 0.7°$
$\sphericalangle(\Phi_{xx}^{(3)}$, bisector of the molecule)	$= 2.2°$

one of the water molecules ($D^{(3)}-O_w^{(2)}-D^{(4)}$) belonging to the octahedron around Al^{3+} is depicted. This figure shows all features of the hydrogen network in the α-alums. The numbering of the atoms is the same as in [17] and will be used throughout this paper. The H-bond lengths D ··· O given in Fig. 7 have been obtained by taking the difference between the O ··· O distances from the data of the protonated Rb-alum [16] and the ND_4-alum [17] into account. The corresponding O–D bond lengths are from the neutron diffraction data of the ND_4-alum. Neutron diffraction data for the Rb-alum are not yet availble.

For "static" D_2O molecules the Φ_{zz} axes are nearly parallel to the corresponding bond directions O–D. A comparison of the respective direction cosines reveals that the "static" D_2O molecules build up the octahedron around the Al^{3+} ions. In Table 3 the assignment of the two EFG tensors to the two deuterons within one D_2O molecule is given together with the bond angle and the whole orientation of the EFG tensors with respect to the molecule. As can been seen, $\Phi_{jj}^{(2)}$ belongs to $D^{(3)}$ and $\Phi_{jj}^{(1)}$, $j=x, y, z$, to $D^{(4)}$. As can be seen from Table 3, the angle $\sphericalangle(\Phi_{zz}^{(1)}, \Phi_{zz}^{(2)}) = 111.8°$ is considerably larger than the "classical" bond angle of 108.2°. The angle formed by the oxygen atoms involved in the H-bond $\sphericalangle(O_w^{(1)}-O_w^{(2)}-O_s^{(2)}) = 101.8°$ (Fig. 7) is even smaller. The two axes $\Phi_{yy}^{(j)}$, $j=1, 2$, deviate only little from the "ideal" orientation $\Phi_{yy} \parallel$ to the normal of molecular plane.

The "flipping" molecules consequently form the distorted water octahedron around Rb^+. In this case $\Phi_{zz}^{(3)}$ is in first approximation perpendicular to the molecular plane of the water molecules (see Table 4). The observed orientation of the EFG tensor with respect to the molecule is in agreement with a model developed by Ketudat [13] and Soda and Chiba [18] for a correlation between the bond angle D–O–D, the asymmetry parameter $\eta(^2H)$, and the orientation of Φ_{jj}, $j=x, y, z$ with respect to the molecule.

There exists a correlation between $eQ\Phi_{zz}h^{-1}(^2H)$ of "static" D_2O molecules and the H-bond length. Several equations which rationalize this empirical finding are given in [18, 19]. All of these equations lead to similar results, and we have chosen the one given by Berglund et al. [19] of the form

$$eQ\Phi_{zz}h^{-1}(^2H) = 303 - 521/d^3(D \cdots O), \quad (1)$$

which has been established by those authors on the basis of experimental data for 13 crystal hydrates. Using the above equation and the D ··· O distances

shown in Fig. 7, the values given in Table 5 have been obtained.

It may be pointed out that there is a considerable difference between the coupling constants of $D^{(3)}$ and $D^{(4)}$, which is not reflected by the values calculated with the aid of (1). Molecular librations leading to a partial averaging of the coupling constants can be responsible for the difference between observed and calculated values in the case of $D^{(3)}$ because the measurements have been carried out at room temperature. In first approximation the coupling constant of $D^{(4)}$ should be affected in the same way. So it is surprising that the coupling constant of $D^{(4)}$ found by NMR is even higher than the one calculated using the H-bond length, indicating that the H-bond is weaker than one expects from the structure. This may be due to the following facts: First, the H-bond involving $D^{(4)}$ points towards a sulphate oxygen and not to a water oxygen like in the case of $D^{(3)}$ (see Figure 7). Secondly the sulphate oxygen $O_s^{(2)}$ is involved in two H-bonds (bifurcated hydrogen bond) and this may weaken the H-bond involving $D^{(4)}$.

The fact that the "static" D_2O molecules belong to the water octahedron around the ion Al^{3+} and the "flipping" ones to the ion Rb^+ is in accordance with the assumption that the electrostatic interaction between the lone pairs of the water oxygen and the central ion is stronger for the higher charged Al^{3+} and the shorter aluminum–oxygen distance ($d(Al^{3+}\cdots O_w^{(2)}) = 192.3$ pm; $d(Rb^+\cdots O_w^{(1)}) = 306.8$ pm). This causes a stronger polarisation of the water molecules which results in a shorter and stronger H-bond and is clearly indicated by the length of the two H-bonds going from different water molecules to the same sulphate oxygen $O_s^{(2)}$ (see Figure 7). For the water molecules surrounding Al^{3+}, the H-bonds are therefore strong enough to prevent a flipping of the molecules even at room temperature.

It would be interesting to check if the $1/d^3(D\cdots O)$ dependence (see (1)) holds for the "flipping" D_2O molecules, too. To do so, we have calculated an average value of a "static" coupling constant for the two deuterons from the parameters of the "flipping" molecules using the already mentioned model by Ketudat [11] and by Soda and Chiba [18]. The results for three different values of $\eta_s(^2H)\cos 2\beta = 0$, 0.1, 0.2 are $eQ\Phi_{zz}h^{-1}(^2H)$ ("static") = 244.2 kHz, 222.0 kHz, 203.5 kHz. Here $\eta_s(^2H)$ is the asymmetry parameter belonging to a static O–D bond and β is the angle between $\Phi_{zz}^{(3)}$ and the normal $\boldsymbol{n}^{(1)}$ of the molecular plane of the water molecule $D^{(1)}$–$O^{(1)}$–$D^{(2)}$. Since β is 2.2° in our case (Table 4) and $\eta_s(^2H)$ is always close to 0.1, the calculated value of 222.0 kHz seems to be the most reasonable one. As can be seen from Table 5 the agreement is surprisingly good.

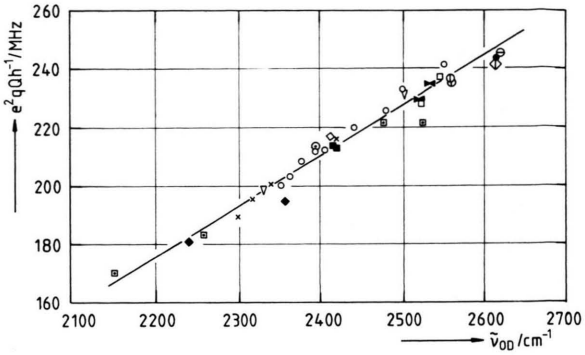

Fig. 8. Plot of $eQ\Phi_{zz}h^{-1}(^2H)$ versus $\tilde{\nu}_{OD}$ for a number of crystal hydrates (see [12]). The data of this work are indicated as ⊡. For the meaning of the other symbols see [12].

Table 5. Hydrogen bond distances D ··· O taken from literature (see text) and quadrupole coupling constants $eQ\Phi_{zz}h^{-1}$ calculated with the aid of (1). O_s, O_w are sulphate-oxygens and D_2O-oxygens, respectively.

Hydrogen bond	Distance pm	$eQ\Phi_{zz}h^{-1}(^2H)_{calc}$ kHz	$eQ\Phi_{zz}h^{-1}(^2H)_{exp}$ kHz
$D^{(1)}\cdots O_s^{(1)}$	195.5	233.3	222.0 *
$D^{(2)}\cdots O_s^{(2)}$	178.5	211.4	222.0 *
$D^{(4)}\cdots O_s^{(2)}$	157.9	170.7	186.5
$D^{(3)}\cdots O_w^{(1)}$	161.0	178.2	169.7

* Calculated from the value for the "flipping" molecule (see text).

Table 6. Comparison of calculated, (2), $\tilde{\nu}_{OD}$(calc.) and measured $\tilde{\nu}_{OD}$(exp.) for O–D stretching vibrations. Values $\tilde{\nu}_{OD}$(Lit.) for the alum $CsAl(SeO_4)_2\cdot 12D_2O$ [25] are given, too.

$eQ\Phi_{zz}h^{-1}$ kHz	$\tilde{\nu}_{OD}$(calc.) cm^{-1}	$\tilde{\nu}_{OD}$(exp.) cm^{-1}	$\tilde{\nu}_{OD}$(Lit.) cm^{-1}
			1780
169.7	2166	2145	2100
186.5	2263	2235	2285
222.0 *	2467	2470	
222.0 *	2467	2525	2540

* Calculated from the value for the "flipping" molecule (see text).

Another valuable parameter in studying H-bonds is provided by the stretching vibration frequencies. The relation between the distances $d(O_w \cdots O)$, $d(O \cdots H)$, and $d(O-H)$ and IR stretching frequencies was recognised by Rundle et al. [20, 21], by Hartert and Glemser [22] and others (see [23]). Blinc and Hadzi [24] pointed out that the values of $eQ\Phi_{zz}h^{-1}(^2H)$ show a correlation with the stretching frequencies in hydrated crystals and other solids containing O–D groups. Berglund et al. [19] have been successful in correlating $\tilde{\nu}_{OD}$ and $\tilde{\nu}_{OH}$ with $eQ\Phi_{zz}h^{-1}$ in crystal hydrates. They report the following equation for "static" D_2O molecules:

$$eQ\Phi_{zz}h^{-1}(^2H) = 0.173 \cdot \tilde{\nu}_{OD} - 205\,. \qquad (2)$$

We have investigated the IR spectra of $RbAl(SO_4)_2 \cdot 12(H_{1-x}D_x)_2O$ for $0.1 \leqq x \leqq 1$ and determined $\tilde{\nu}_{OD}$. The results are given in Table 6 together with values reported by Petrov et al. [25] for $CsGa(SeO_4)_2 \cdot 12\,D_2O$, which most probably belongs to the α-alums since for example $CsAl(SO_4)_2 \cdot 12\,H_2O$ is a β-alum while $CsAl(SeO_4)_2 \cdot 12\,H_2O$ an α-alum [8]. In Fig. 8 a plot of $eQ\Phi_{zz}h^{-1}(^2D)$ versus $\tilde{\nu}_{OD}$ according to [12] is depicted. It turns out that the value of 1780 cm^{-1} given by Petrov et al. does not fit into that plot by any means and seems to be in error. We could not obtain any signal in that region. Furthermore one can see that the calculated value of the average coupling constant for $D^{(1)}$ and $D^{(2)}$ for a "static" molecule fits very well into the scheme, and that an assignment of the O–D stretching frequencies to the different water molecules and for the "static" molecules even to the different O–D bonds is possible. The rather low value of $eQ\Phi_{zz}h^{-1}(^2H) = 169.7$ kHz obtained for $D^{(3)}$ extends the curve considerably to lower values of $\tilde{\nu}_{OD}$.

We are grateful to the Stiftung Volkswagenwerk for financial support of this work. One of us, J. Ramakrishna, thanks the Alexander von Humboldt Foundation for support.

[1] W. C. Bailey and H. S. Story, J. Chem. Phys. **58,** 1255 (1973).
[2] G. Burns, J. Chem. Phys. **32,** 64 (1961).
[3] W. G. Segleken and H. C. Toorey, Phys. Rev. **98,** 1537 (1955).
[4] H. S. Story, W. Bailey, and D. Kline, Bull. Amer. Chem. Soc. **13,** 885 (1968).
[5] I. S. Vinogradova, Sov. Phys.-Solid State **10,** 1727 (1969).
[6] I. S. Vinogradova and L. G. Falaleeva, Bull. Acad. Sci. USSR **33,** 231 (1969).
[7] N. Weiden and Al. Weiss, Ber. Bunsenges. Phys. Chem. **78,** 1031 (1974).
[8] N. Weiden and Al. Weiss, Ber. Bunsenges. Phys. Chem. **79,** 557 (1975).
[9] N. Weiden and Al. Weiss, J. Magn. Reson. **20,** 279 (1975).
[10] G. E. Pake, J. Chem. Phys. **16,** 327 (1948).
[11] S. Ketudat and R. V. Pound, J. Chem. Phys. **26,** 708 (1957).
[12] Al. Weiss and N. Weiden, Adv. Nucl. Quadrupole Reson. **4,** 149 (1980).
[13] S. Ketudat, Thesis, Havard University 1957.
[14] G. M. Volkoff, H. E. Petch, and D. W. L. Smellie, Canad. J. Phys. **30,** 270 (1952).
[15] G. Hutton and B. Pedersen, J. Magn. Reson. **13,** 119 (1974).
[16] A. C. Larson and D. T. Cromer, Acta Cryst. **22,** 793 (1967).
[17] D. T. Cromer and M. I. Kay, Acta Cryst. **22,** 800 (1967).
[18] G. Soda and T. Chiba, J. Chem. Phys. **50,** 439 (1969).
[19] B. Berglund, J. Lindgren, and J. Tegenfeldt, J. Mol. Struct. **43,** 179 (1978).
[20] R. E. Rundle and M. Parasol, J. Chem. Phys. **20,** 1487 (1952).
[21] K. Nakamoto, M. Margoshes, and R. E. Rundle, J. Amer. Chem. Soc. **77,** 6480 (1955).
[22] E. Hartert and O. Glemser, Naturwiss. **40,** 199, 552 (1953).
[23] S. N. Vinogradov and R. H. Linell, Hydrogen Bonding, Van Nostrand Reinhold Co., New York 1971.
[24] R. Blinc and D. Hadzi, Nature London **212,** 1307 (1966).
[25] K. I. Petrov, N. K. Bol'shakova, V. V. Kravchenko, and L. D. Iskhakova, Russ. J. Inorg. Chem. **15,** 1529 (1970).